

**Terahertz (THz) Catalysis on MXene for Enhanced Selectivity from CO<sub>2</sub> to CO**

*Ziao Wang<sup>1</sup>, Yao Xu, Tao Feng<sup>2</sup>, Chaojun Lei<sup>2</sup>, Yu Zhao<sup>2\*</sup> and Xi Zhu<sup>1\*</sup>*

<sup>1</sup>Shenzhen Institute of Artificial Intelligence and Robotics for Society (AIRS),

The Chinese University of Hong Kong, Shenzhen (CUHK-Shenzhen),

Shenzhen, Guangdong, P. R. China. 518172

Email: [zhuxi@cuhk.edu.cn](mailto:zhuxi@cuhk.edu.cn)

<sup>2</sup>College of Material, Chemistry and Chemical Engineering,

Key Laboratory of Organosilicon Chemistry and Material Technology,

Ministry of Education, Hangzhou Normal University,

Hangzhou, Zhejiang, P. R. China. 311121

Email: [yuzhao@suda.edu.cn](mailto:yuzhao@suda.edu.cn)

This supplementary information file includes:

- Supplementary Notes 1 - 5
- Supplementary Figures 1 - 9
- Supplementary Tables 1
- Supplementary References

### **Supplementary Note 1 Materials**

Ti<sub>3</sub>AlC<sub>2</sub> (Jilin Eleven Technology), hydrochloric acid (HCl, technical grade), hydrofluoric acid (HF, Sigma Aldrich), sodium hydroxide (NaOH, technical grade) were used.

### **Supplementary Note 2 Synthesis of Ti<sub>3</sub>C<sub>2</sub>F<sub>2</sub> MXene**

Ti<sub>3</sub>C<sub>2</sub>T<sub>x</sub> MXenes were synthesized by selectively etching Al atoms from Ti<sub>3</sub>AlC<sub>2</sub> using HF/HCl etchant. Briefly, 12 mL of hydrochloric acid (HCl, 35-38%), 2.5 mL of hydrofluoric acid (HF, 40%), and 6 mL of deionized water were mixed by stirring. Then 1 g of Ti<sub>3</sub>AlC<sub>2</sub> was slowly added to the solution at 35°C, followed by stirring at 400 rpm for 24 hours. The resulting suspension (multilayer MXene) was washed with deionized (DI) water by centrifugation at 5000 rpm (5 min per cycle) until pH ≥ 6. The precipitate was collected and redispersed in 20 mL of water, then the multilayer dispersion was added and centrifuged with deionized water at 7000 rpm until pH ≥ 6. In addition, the pellet was redispersed into a small amount of deionized water, and the highly concentrated supernatant containing layered monolayers and oligomeric Ti<sub>3</sub>C<sub>2</sub>T<sub>x</sub> MXene flakes was collected by centrifugation at 5000 rpm. The concentration of the Ti<sub>3</sub>C<sub>2</sub>T<sub>x</sub> dispersion was vacuum dried at 70 °C overnight, and the weight of the solid residue was measured. Robotic arms automate all solution movement.

### **Supplementary Note 3 Alkaline treatment of MXene**

Alkaline treatment of Ti<sub>3</sub>C<sub>2</sub>T<sub>x</sub> MXenes was achieved by mixing MXene with concentrated sodium hydroxide (NaOH) solution. Take 0.2 g of MXene prepared by the above synthesis method, dissolve it in 10 mL of distilled water, and stir and mix with 1 mol/L NaOH solution at 80°C under magnetic stirring at 300 rpm for 1h. After filtration and washing with distilled water until pH ≤ 8, it is dried in a vacuum oven at 60°C. Dry the LiOH-treated powder in a vacuum oven at 60°C for 12 hours.

### **Supplementary Note 4 Characterization**

X-ray diffraction (XRD) was performed on a Bruker D8 Advance powder X-ray diffractometer equipped with copper K $\alpha$  radiation ( $\lambda=1.540598 \text{ \AA}$ ). Raman spectra were recorded with a Raman microscope equipped with a 532 nm laser, 600-line mm<sup>-1</sup> grating, 10% laser power, and a 50x objective. Spectra were acquired with a dwell time of 90 seconds and 2 accumulations. The morphology and microstructure of the samples were described by scanning electron microscopy (SEM) (Tescan Mira 3). The chemical composition of the samples was analyzed by high-resolution X-ray photoelectron spectroscopy (XPS, thermal K- $\alpha$ ), multi-channel plate, and delay line Detector,  $2 \times 10^{-9}$  mbar vacuum. The samples were mounted in floating mode to avoid differential charging. Charge neutralization is required for all samples. Using the C 1s peak of the (C-C) bond as a reference, the binding energy was set to 284.8 eV.

### **Supplementary Note 5 Computational Details**

All density functional theory (DFT) calculations were performed by using the Vienna ab initio simulation package (VASP).<sup>1</sup> Exchange-correlation interactions were described by the generalized gradient approximation (GGA) parameterized by the Perdew-Burke-Ernzerhof (PBE) method.<sup>2</sup> Van der Waals (vdW) interactions were accounted for by using the DFT-D3 scheme.<sup>3, 4</sup> The energy cutoff of the plane wave base was set to 500 eV, and the  $3 \times 3 \times 1$  k point grid is sampled using the Monkhorst-Pack method,<sup>5</sup> which provided sufficient accuracy for Brillouin zone integration. By using the conjugate gradient (CG) algorithm, all structures were completely relaxed until the force was less than 0.005 eV/ $\text{\AA}$  and the energy change was less than  $10^{-8}$  eV. To simulate the surface of MXene ( $\text{Ti}_3\text{C}_2\text{F}_2$ ), we used a  $2 \times 2 \times 1$  monolayer supercell and cut the crystal along the (0 0 1) direction. The vacuum region in the z-direction was set to 15  $\text{\AA}$  to avoid interactions between the layers. In the THz irradiation condition, we changed corresponding bond length, according to calculated vibrational spectrum, to simulate irradiated MXene surface.

### **Supplementary Note 6 Natural Language Processing Algorithm**

The brief workflow of the Natural Language Processing (NLP) application is shown in Supplementary Figure S10. Preparing the input text for easier analysis is the first critical step. Therefore, establishing a database with good data quality and sufficient quantity is essential in NLP-based data mining work. We used a similar data collection pipeline developed by Kim et al.<sup>6</sup> to download a large number of papers related to catalysis published after 2011 in HTML/XML format from the publisher's website and transfer them to PDF versions. We chose 2011 as the cut-off year because we wanted to use a 10-year timeline for our study, and 2011 happens to be the year when MXene was first synthesized. The information of articles, such as journal name, article title, author's name, etc., are listed in Supplementary File 1. To date, we have accumulated 75.5 thousand of articles that will be used for subsequent processing.

The experimental paragraph classification method is the semi-supervised random forest (RF) model from Huo et al.<sup>7</sup>. We used the Bi-LSTM neural network with a conditional random field layer to extract the word-level labels (e.g., reaction type, reaction condition, reactant, catalyst, irrelevant word) introduced by He et al.<sup>8</sup>. Summing all word representations, averaging, and combining word representations into sentence representations can be done by summation, i.e., summing all word representations, averaging, etc. Still, these methods do not consider the order of the words before and after in the sentence. Longer distance dependencies can be better captured using the LSTM model. But one more problem with modeling sentences using LSTM is the inability to encode information from back to front. The bi-directional semantic dependencies can be better captured by Bi-LSTM.

The Word2Vec algorithm uses a neural network model to learn word associations from a large text corpus.<sup>9</sup> We implemented an algorithm that combines neural networks and sentence dependency tree analysis to identify synthetic actions in the text. First, the Word2Vec model was retrained on approximately 79,500 experimental methods paragraph passages. These word embeddings were used to input a recurrent neural network that takes a sentence word by word and assigns labels to different categories.

For reaction, the labels were set as HER, OER, ORR, NRR, and CO<sub>2</sub>RR. The labels of reaction conditions were: ultraviolet, photo, infrared, Terahertz (THz), microwave, or heating. We use the rule-based regular expression method to extract the corresponding values for these attributes.<sup>10</sup> Articles that applied the same or similar conditions would be categorized and organized.

Meanwhile, articles with inconsistent reaction conditions and reaction types are deleted from the database by analyzing the combinations of keywords. The experimental conditions or wavelength units are first located in the paragraphs of the catalytic experimental procedure by keyword search. The collected keywords for the experimental conditions are directly sorted for the next data step. If the wavelength unit is filtered, the corresponding number is found from the front of the word and merged with the unit to determine the wavelength used for that experiment. Collate the wavelengths corresponding to the preset experimental method lexicon.

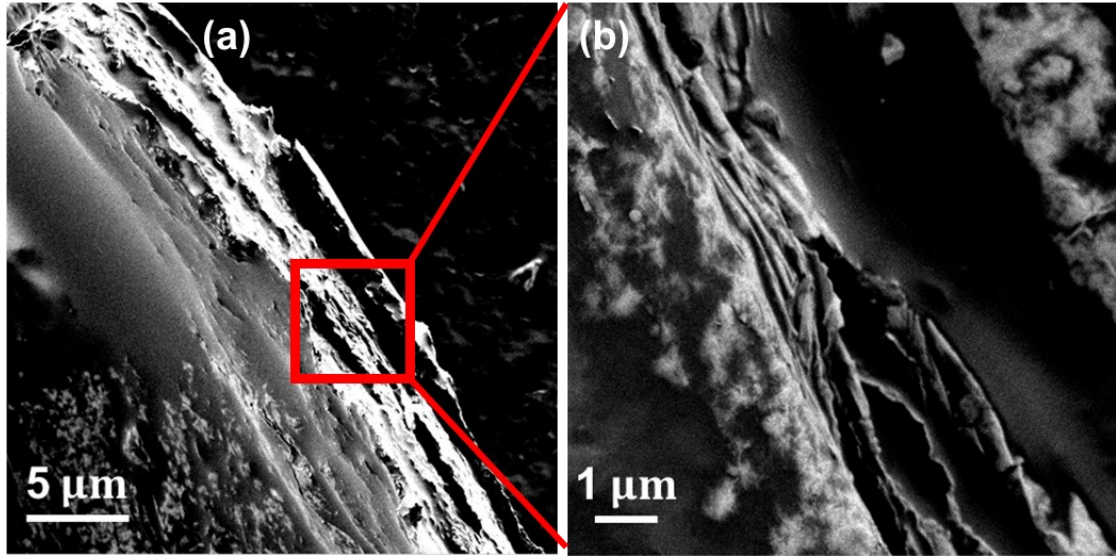


**Figure S1** The SEM image of automatic synthesized MXene layered structure with **(a)**  $5\ \mu\text{m}$  and **(b)**  $1\ \mu\text{m}$

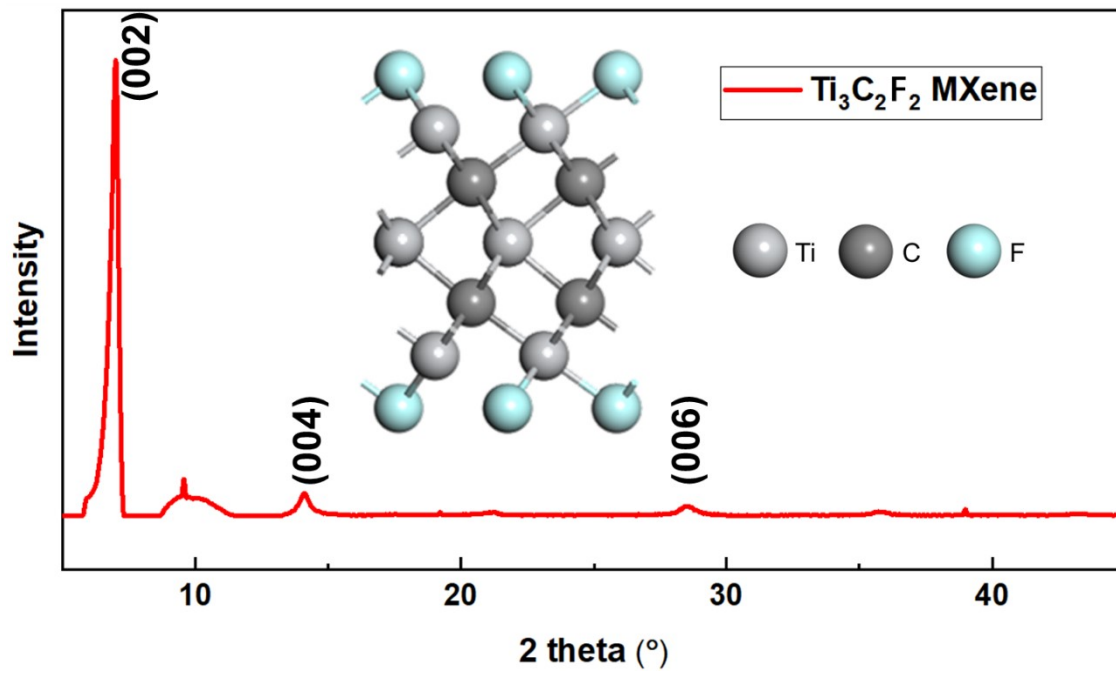


**Figure S2** The XRD image and the molecular structure of  $\text{Ti}_3\text{C}_2\text{F}_2$  MXene.

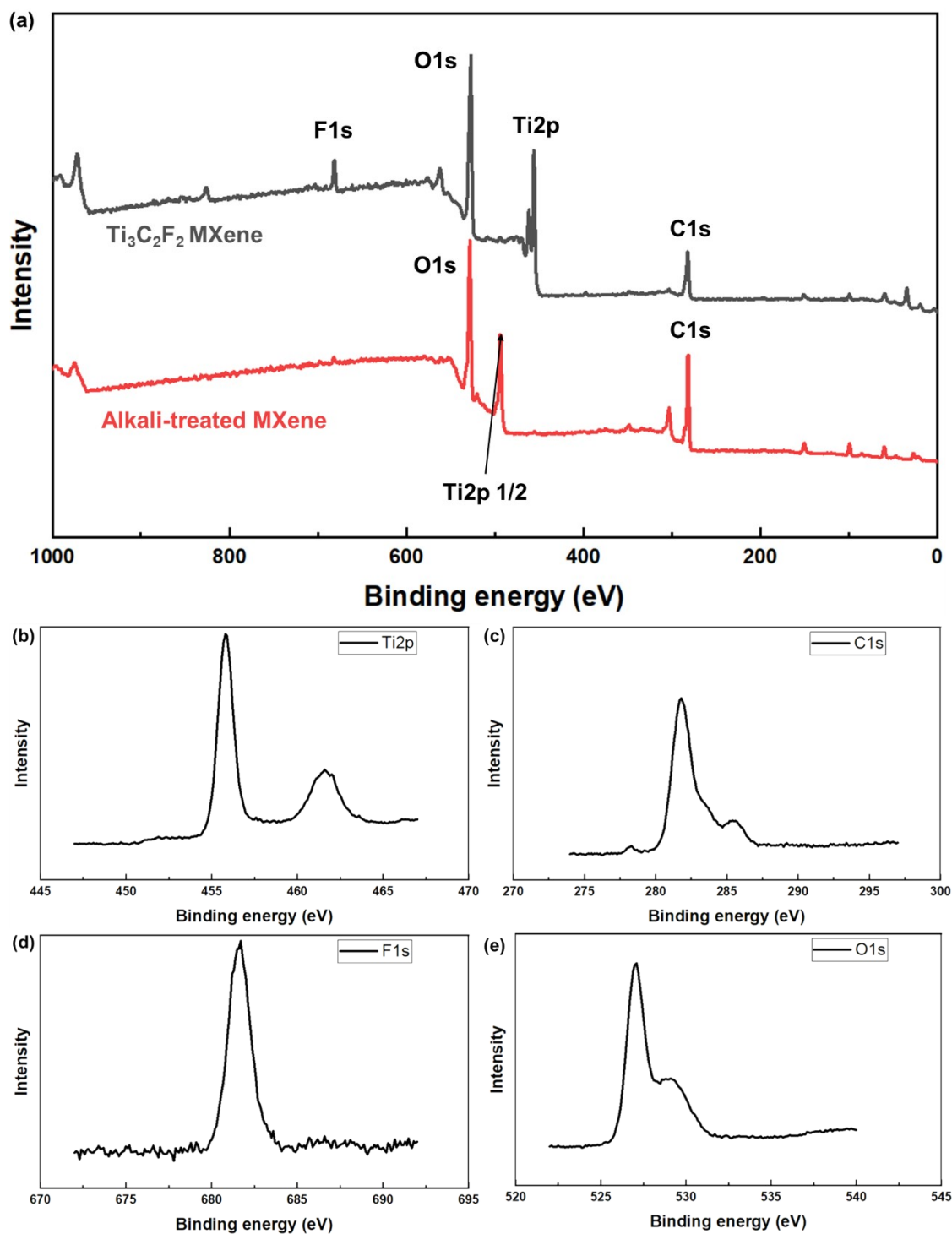


**Figure S3** (a) Full XPS spectra of two kinds of powder High-resolution spectra of (b) Ti2p on the upper left, (c) C1s on the upper right, (d) F1s on the lower left, and (e) O1s on lower right regions



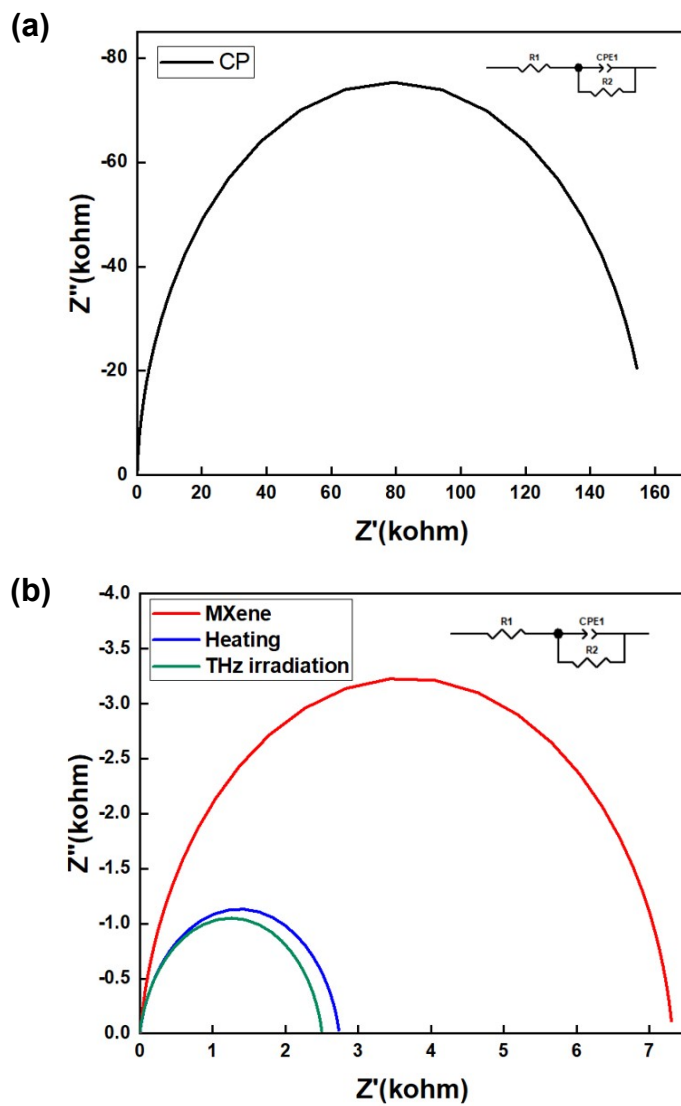


**Figure S4** (a) EIS Nyquist plots of bare carbon paper (CP). (b) EIS Nyquist plots of bare MXene, MXene under heating, and MXene under THz irradiation.

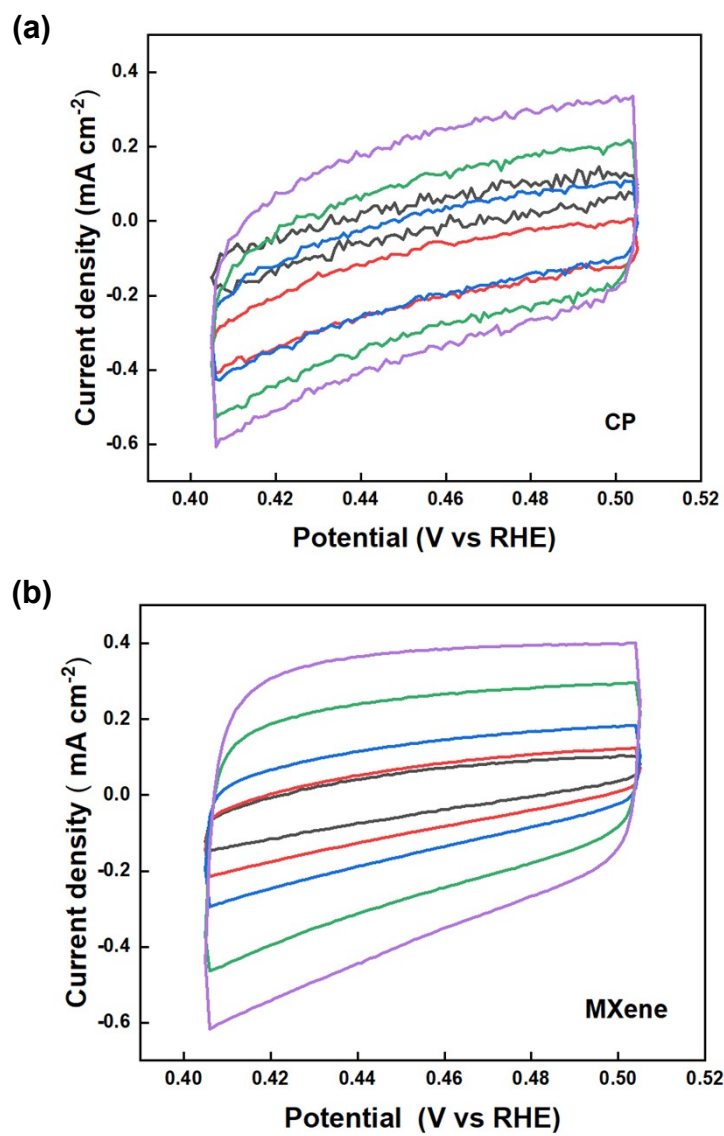


**Figure S5** (a) CV curves of the CP, and (b) CV curves of the MXene electrocatalyst obtained at different scan rates in 0.5 M H<sub>2</sub>SO<sub>4</sub>.

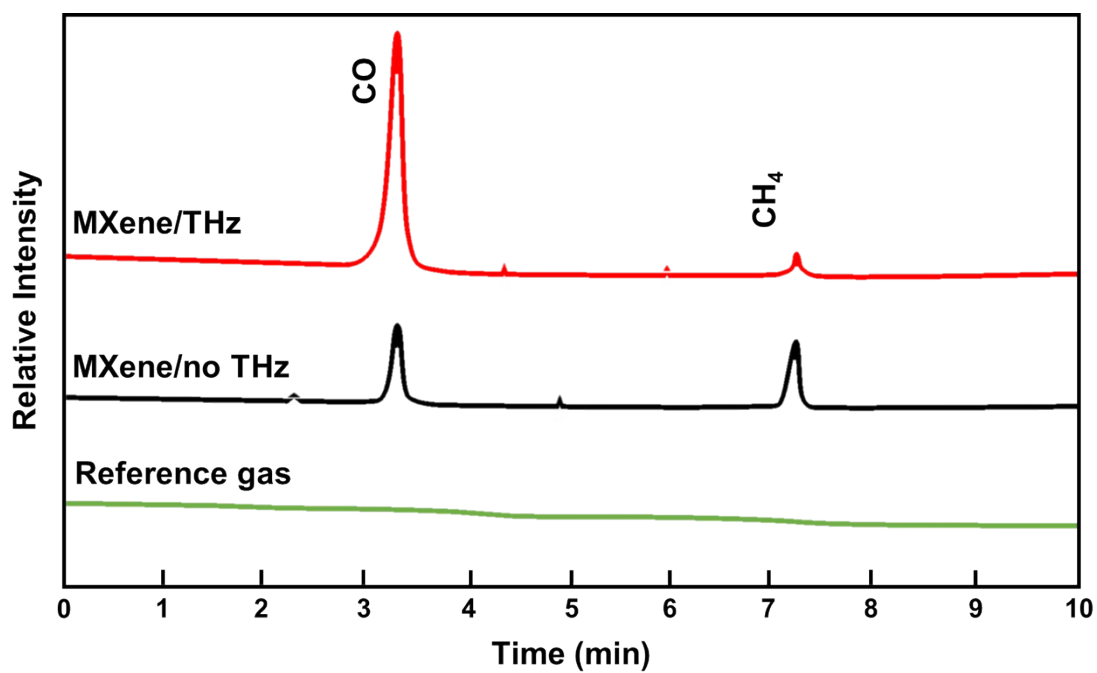


**Figure S6** Comparison of the gas chromatograms for the gaseous products of electrochemical CO<sub>2</sub>RR process with different conditions (with or without THz irradiation).

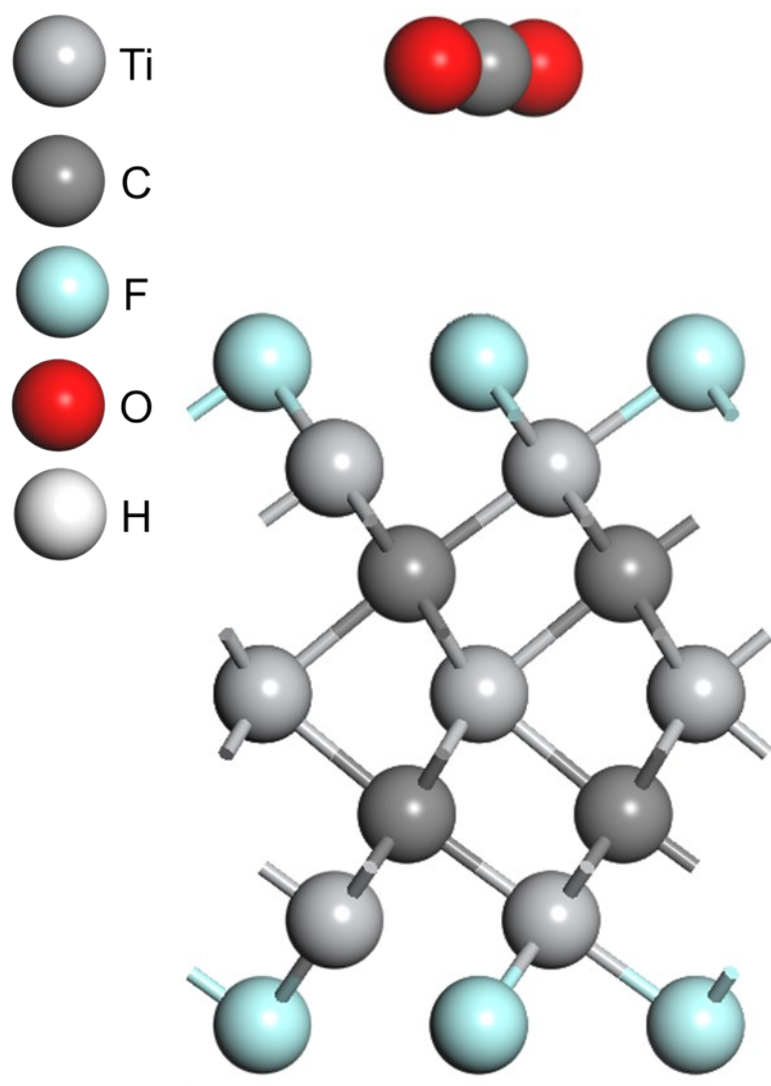


**Figure S7** The structure model of a CO<sub>2</sub> molecule on the Ti<sub>3</sub>C<sub>2</sub>F<sub>2</sub> MXene surface, with the red, dark grey, grey, and light blue ball O, C, Ti, and F atoms, respectively.

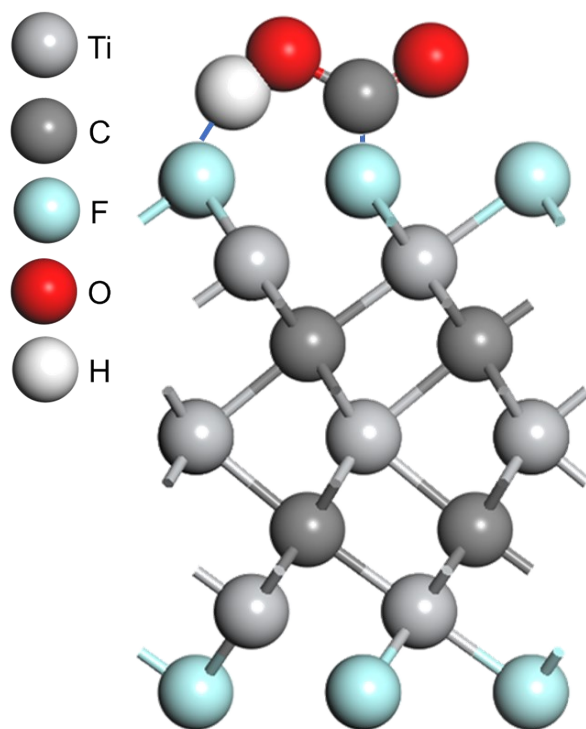


**Figure S8** The structure model of a \*COOH group on the Ti<sub>3</sub>C<sub>2</sub>F<sub>2</sub> MXene surface, with the red, dark grey, grey, and light blue ball O, C, Ti, and F atoms, respectively.

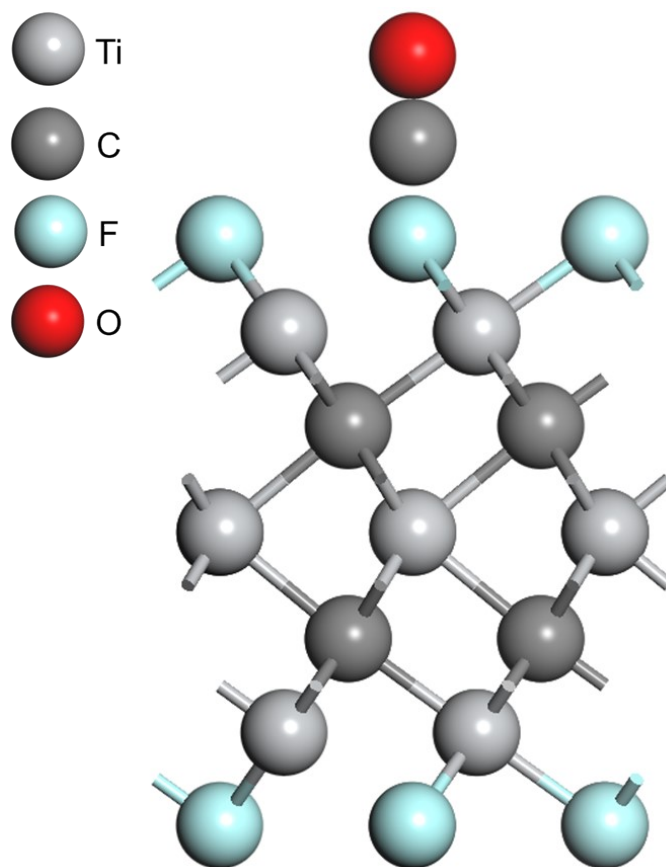


**Figure S9** The structure model of a \*CO group on the  $\text{Ti}_3\text{C}_2\text{F}_2$  MXene surface, with the red, dark grey, grey, and light blue ball O, C, Ti, and F atoms, respectively.

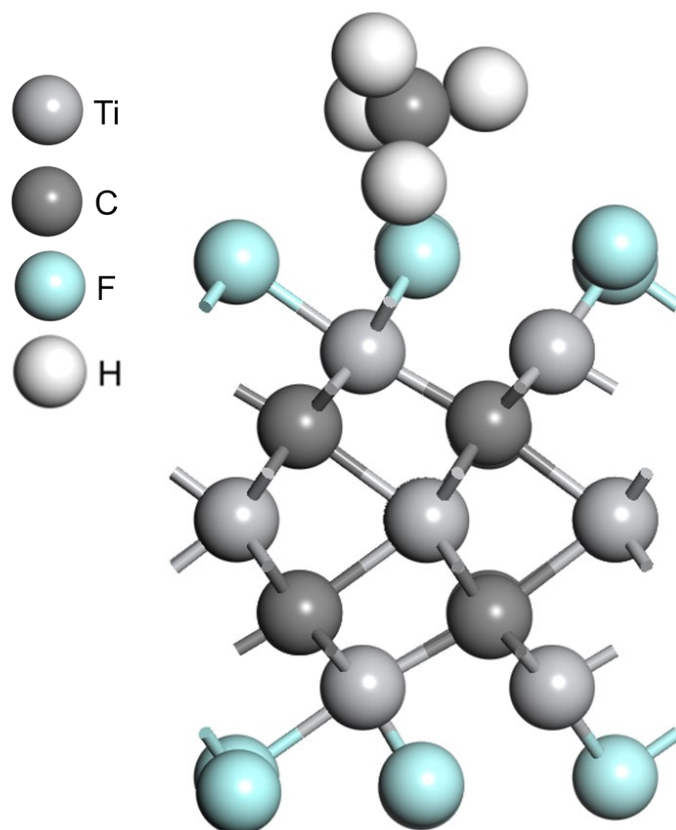


**Figure S10** The structure model of a  $\text{CH}_4$  molecule on the  $\text{Ti}_3\text{C}_2\text{F}_2$  MXene surface, with the red, dark grey, grey, and light blue balls O, C, Ti, and F atoms, respectively.

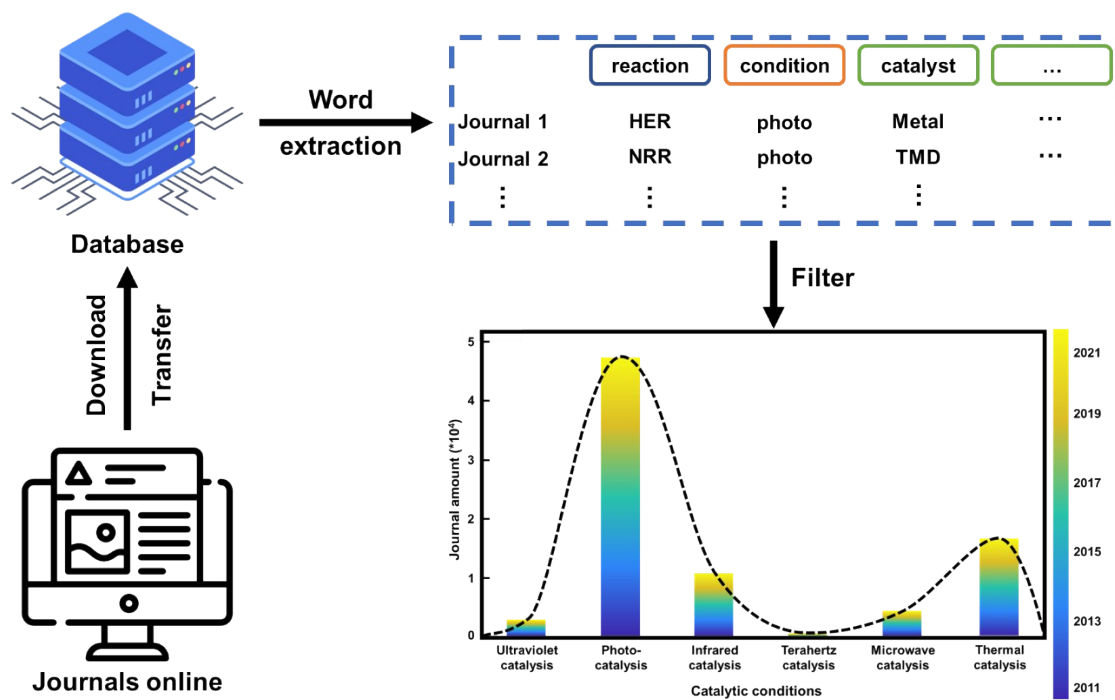


Figure S11 The brief workflow of the application of NLP.



**Table S1. Comparison of the product ratio of CO and CH<sub>4</sub> for different conditions in this work and other works.**

<i>Electrode</i>	<i>CO in product</i>	<i>CH<sub>4</sub> in product</i>	<i>Reference</i>
<i>MXene/THz</i>	86.44%	13.32%	This work
<i>MXene/no THz</i>	48.40%	31.42%	This work
<i>P25/MXene</i>	41.41%	58.59%	11
<i>CsPbBr<sub>3</sub>/MXene</i>	78.40%	21.60%	12
<i>TiO<sub>2</sub>/C<sub>3</sub>N<sub>4</sub>/MXene</i>	78.53%	21.47%	13

**Supplementary File 1 NLP.txt**

This supplementary file is the collection of information of articles we used in NLP analysis, such as journal name, article title, author's name, etc.

## References

1. Kresse, G.; Furthmüller, J., Efficient iterative schemes for ab initio total-energy calculations using a plane-wave basis set. *Physical review B* **1996**, *54*, 11169.
2. Perdew, J. P.; Burke, K.; Ernzerhof, M., Generalized gradient approximation made simple. *Physical review letters* **1996**, *77*, 3865.
3. Blöchl, P. E., Projector augmented-wave method. *Physical review B* **1994**, *50*, 17953.
4. Payne, M. C.; Teter, M. P.; Allan, D. C.; Arias, T.; Joannopoulos, a. J., Iterative minimization techniques for ab initio total-energy calculations: molecular dynamics and conjugate gradients. *Reviews of modern physics* **1992**, *64*, 1045.
5. Moellmann, J.; Grimme, S., DFT-D3 study of some molecular crystals. *The Journal of Physical Chemistry C* **2014**, *118*, 7615-7621.
6. Kim, E.; Huang, K.; Tomala, A.; Matthews, S.; Strubell, E.; Saunders, A.; McCallum, A.; Olivetti, E., Machine-learned and codified synthesis parameters of oxide materials. *Scientific data* **2017**, *4*, 1-9.
7. Huo, H. Y.; Rong, Z. Q.; Kononova, O.; Sun, W. H.; Botari, T.; He, T. J.; Tshitoyan, V.; Ceder, G., Semi-supervised machine-learning classification of materials synthesis procedures. *Npj Computational Materials* **2019**, *5*.
8. He, T.; Sun, W.; Huo, H.; Kononova, O.; Rong, Z.; Tshitoyan, V.; Botari, T.; Ceder, G., Similarity of precursors in solid-state synthesis as text-mined from scientific literature. *Chemistry of Materials* **2020**, *32*, 7861-7873.
9. Mikolov, T.; Chen, K.; Corrado, G.; Dean, J., Efficient estimation of word representations in vector space. *arXiv preprint arXiv:1301.3781* **2013**.
10. Jurafsky, D.; Martin, J. H., *Speech and Language Processing: An Introduction to Natural Language Processing, Computational Linguistics, and Speech Recognition*.
11. Ye, M. H.; Wang, X.; Liu, E. Z.; Ye, J. H.; Wang, D. F., Boosting the Photocatalytic Activity of P25 for Carbon Dioxide Reduction by using a Surface-Alkalinized Titanium Carbide MXene as Cocatalyst. *Chemsuschem* **2018**, *11*, 1606-1611.
12. Pan, A.; Ma, X.; Huang, S.; Wu, Y.; Jia, M.; Shi, Y.; Liu, Y.; Wangyang, P.; He, L.; Liu, Y., CsPbBr<sub>3</sub> Perovskite Nanocrystal Grown on MXene Nanosheets for Enhanced Photoelectric Detection and Photocatalytic CO<sub>2</sub> Reduction. *J Phys Chem Lett* **2019**, *10*, 6590-6597.
13. He, F.; Zhu, B.; Cheng, B.; Yu, J.; Ho, W.; Macyk, W., 2D/2D/0D TiO<sub>2</sub>/C<sub>3</sub>N<sub>4</sub>/Ti<sub>3</sub>C<sub>2</sub> MXene composite S-scheme photocatalyst with enhanced CO<sub>2</sub> reduction activity. *Applied Catalysis B: Environmental* **2020**, *272*, 119006.